

van Hove Singularity Induced $L1_1$ Ordering in CuPt

J. F. Clark,¹ F. J. Pinski,¹ D. D. Johnson,² P. A. Sterne,³ J. B. Staunton,⁴ and B. Ginatempo⁵

¹*Department of Physics, University of Cincinnati, Cincinnati, Ohio 45221*

²*Computational Materials Science Department, MS 9161, Sandia National Laboratories, Livermore, California 94551*

³*Department of Physics, University of California, Davis, California 95616*

and Department of Chemistry and Materials Science, L-268, Lawrence Livermore National Laboratory, Livermore, California 94551

⁴*Department of Physics, University of Warwick, Coventry CV7 4AL, United Kingdom*

⁵*Istituto di Fisica Teorica, Università di Messina, Messina, Italy*

(Received 6 June 1994)

We describe an ordering mechanism that arises due to coupling between electronic states at van Hove singularities. This novel mechanism, which naturally leads to ordered structures with small unit cells, couples states near the Fermi energy which are localized at high-symmetry points in \mathbf{k} space, in contrast to the conventional mechanism which relies on large parallel sheets of Fermi surface. Using first-principles calculations of the electronic structure of ordered and disordered alloys, we show that this mechanism drives the unusual short- and long-range order found in fcc CuPt.

PACS numbers: 71.20.Cf, 64.60.Cn, 75.40.Cx

CuPt is the only metallic alloy which forms in the $L1_1$ structure [1]. This structure consists of alternating fcc (1, 1, 1) layers of Cu and Pt, in contrast with the more common $L1_0$ structure which has alternating (1, 0, 0) planes of atoms. In this Letter, we describe the novel origin for the structural ordering observed in CuPt. We show that the $L1_1$ structure is stabilized by a Peierls-like mechanism arising from the hybridization between van Hove singularities at the high-symmetry X and L points in the fcc Brillouin zone. This mechanism naturally leads to ordered structures with small unit cells, commensurate with the underlying fcc lattice, and could also explain the stability of such structures in other systems. In contrast, the more conventional Fermi-surface-nesting mechanism typically leads to long-period superstructures (LPS), which are observed in Cu, Ag, and Au rich alloys [1]. $\text{Cu}_{1-c}\text{Pt}_c$ is particularly interesting since by varying the Pt concentration one can observe both the $L1_1$ ordering associated with the proposed mechanism ($c = 0.5$) and the LPS associated with Fermi-surface nesting ($c \approx 0.73$).

We investigate the stability of the disordered solid solution phase of CuPt by calculating the atomic short-range order (ASRO) using a mean-field statistical approach based on a first-principles description of the finite-temperature, electronic grand potential of the disordered alloy. This approach is based on standard Korringa-Kohn-Rostoker coherent-potential-approximation [2–4] (KKR-CPA) electronic-structure formalism. At high temperatures, the calculated ASRO has spectral peaks at the wave vector $(\frac{1}{2}, \frac{1}{2}, \frac{1}{2})$, indicative of the observed low-temperature CuPt $L1_1$ structure [5], in agreement with experiment [6]. It is a strength of this approach that the electronic origin of this ASRO can be determined unambiguously from these calculations. These results are complemented by ordered (zero-temperature) calculations comparing the total energies and densities of states of the $L1_0$ and $L1_1$ structures. These calculations confirm

the lower energy of the $L1_1$ structure, and support the mechanism based on the coupling of high-symmetry points suggested by the ASRO calculations.

For a binary A_cB_{1-c} alloy, any chemical configuration (whether ordered or disordered) can be described by a set of site-occupation variables ξ_i . Here ξ_i is 1 (0) if an A -type atom does (does not) occupy the i th site in the lattice. The thermodynamic average of ξ_i , $\langle \xi_i \rangle$, is then the average concentration (or probability) of an A atom at that site, c_i . At very high temperatures the alloy is (assumed to be) homogeneously disordered and, as such, $c_i = c$ for all sites. By applying small, inhomogeneous “external” chemical potentials $\{\delta\nu_i\}$ to induce changes in the site-occupational probabilities, $\{\delta c_i\}$, we consider the linear response of the atomic pair correlations which develop as the temperature is lowered. The KKR-CPA approach is then appropriate for describing the configurational average over the electronic degrees of freedom for this reference state, and gives a good description of its electronic structure and energetics [3,4,7]. The compositional correlations can then be investigated via the fluctuation-dissipation theorem which connects these responses to the atomic pair-correlation function, $\alpha_{ij} = \delta c_i / \delta \nu_j = \beta (\langle \xi_i \xi_j \rangle - \langle \xi_i \rangle \langle \xi_j \rangle)$, where $\beta = (k_B T)^{-1}$.

In terms of concentration waves, the central result is that the ASRO (or the Fourier transform of the atomic pair-correlation function), which is measured by diffuse scattering experiments, can be written formally [8–10] as

$$\alpha(\mathbf{q}) = \frac{\beta c(1-c)}{1 - \beta c(1-c)[S^{(2)}(\mathbf{q}, c) - \Lambda_c]}, \quad (1)$$

with

$$\Lambda_c = \frac{1}{\beta c(1-c)} \frac{1}{\Omega_{\text{BZ}}} \int d\mathbf{q} S^{(2)}(\mathbf{q}) \alpha(\mathbf{q}),$$

$$S^{(2)}(\mathbf{q}, c) = \mathcal{F} \left[\frac{\partial^2 \Omega^{\text{CPA}}(\{c_i\})}{\partial c_i \partial c_j} \right]_{c_i=c\mathbf{v}_i},$$

where \mathcal{F} refers to a Fourier transform in the random state. Because of the internally consistent use of the mean field for both the electronic-configurational and thermodynamic averaging, only “point” entropy is included in $\alpha(\mathbf{q})$. $S^{(2)}(\mathbf{q})$ provides direct information on the stability of the randomly disordered alloy to concentration fluctuations at temperature T . The \mathbf{q} dependence of $\alpha(\mathbf{q})$, or $S^{(2)}(\mathbf{q})$, depends on details of the random alloy’s electronic structure, and, perhaps, on details of the double-counting contributions. The maxima of $\alpha(\mathbf{q})$ describe the type of ordering (or chemical correlations) in the alloy. In the above equations, Ω^{CPA} is the KKR-CPA electronic grand potential for an inhomogeneous configuration $\{c_i\}$. The Onsager cavity correction Λ_c , which is important for long-ranged interactions, is temperature dependent but wave vector independent, and maintains the spectral intensity over the Brillouin zone, i.e., $\alpha_{ii} = \beta c(1 - c)$ [9–13]. This sum rule is generally not maintained in mean-field theories.

Except for being altered by Onsager corrections, Eq. (1) is analogous to that of Gorsky, Bragg, and Williams [14,15] (or the Krivoglaz-Clapp-Moss formula [16]). However, it is more robust owing to the electronic basis of the theory and its concentration dependence, and, as such, it can give rise to much different behavior than found historically for the Gorsky-Bragg-Williams model [9,10]. Details of this first-principles theory of ASRO were discussed originally by Gyorffy and Stocks [8] and co-workers [12,17] for the case in which only the electronic band energy is considered. More recently, Staunton, Johnson, and Pinski [9,10] have discussed the generalization to include all terms beyond band energy (so-called “double-counting” terms) in the grand potential, as well as the details and importance of the Onsager corrections to mean fields. Notably, there are self-energy corrections [9] to $S^{(2)}(\mathbf{q})$ and Λ_c that are derived on an internally consistent electronic basis, not just via the simple integration.

In the ASRO calculations, all electronic terms are included within the single constraint of a fixed Bravais lattice [9] and all potentials are obtained self-consistently from the scalar-relativistic KKR-CPA, using the local approximation to density-functional theory [18]. For simplicity, the experimental lattice constant of CuPt was used. We note that in fully relativistic calculations the magnitude of ASRO is reduced by at most 10% [19,20], and, therefore, spin-orbit terms have only a small effect.

The importance of this first-principles concentration-wave approach lies in the ability to pinpoint a specific electronic origin of ASRO. This is especially useful when the high-temperature state is a precursor of the low-temperature ordered state, as is the case for CuPt. Our calculated ASRO [19,20] for CuPt indicates an instability to concentration fluctuations with a wave vector of $(\frac{1}{2}, \frac{1}{2}, \frac{1}{2})$, consistent with the observed $L1_1$ ordering [1]. In what follows, we isolate the fundamental electronic features responsible for the observed ASRO and for

the chemical interactions, whether they be ultimately represented in real or reciprocal space. (In real space, the resulting first two neighbor interactions are large and have the same sign, and are sufficient to give the $L1_1$ ground state in a next-neighbor Ising model [21].)

We find that the electron states near the Fermi energy, ϵ_F , play the dominant role in determining the $L1_1$ ordering tendency found from $S^{(2)}(\mathbf{q})$. In such a case, it is instructive to interpret (not calculate) $S^{(2)}(\mathbf{q})$ in terms of the convolution of Bloch spectral functions $A_B(\mathbf{k}; \epsilon)$ as [8,12]

$$\int d\epsilon \int d\epsilon' \frac{f(\epsilon) - f(\epsilon')}{\epsilon - \epsilon'} \int d\mathbf{k} A_B(\mathbf{k}; \epsilon) A_B(\mathbf{k} + \mathbf{q}; \epsilon'), \quad (2)$$

where $f(\epsilon)$ is the Fermi function. For ordered alloys, this reduces to a standard susceptibility form [12]. For an ordered alloy $A_B(\mathbf{k}; \epsilon)$ consists of delta functions in \mathbf{k} space whenever the dispersion relationship is satisfied, i.e., $\delta(\epsilon - \epsilon_{\mathbf{k}})$. In a disordered alloy, these delta functions broaden and shift (in energy) due to the disorder and alloying effects. A disordered alloy’s “Fermi surface” can be described by tracing the loci of peak positions at ϵ_F , if the widths are small on the scale of the Brillouin zone dimension. Peaks in $S^{(2)}(\mathbf{q})$ can arise from states around the ϵ_F in two ways: due to parallel, flat sheets of Fermi surface which give a large convolution as $\epsilon - \epsilon' \rightarrow 0$ (so-called Fermi-surface nesting), or, as described below, due to a large joint density of states connecting van Hove singularities at or near ϵ_F .

As shown in Fig. 1, the Fermi surface of disordered CuPt has a distinctive “neck” feature near the L point similar to elemental Cu. Furthermore, pockets of d holes exist at the X points, since ϵ_F cuts the density of states near the top of a feature that is mainly Pt d in character; see Fig. 2(a). As a result, the joint density of states in Eq. (2), and therefore the ASRO, peaks at $(\frac{1}{2}, \frac{1}{2}, \frac{1}{2})$ due to the large joint electron density of states at $X = (0, 0, 1)$ and $L = (\frac{1}{2}, \frac{1}{2}, \frac{1}{2})$. Notice that the spanning vector $X-L$ is a member of the star of L which is the ordering wave vector for the $L1_1$ ordering tendency [5].

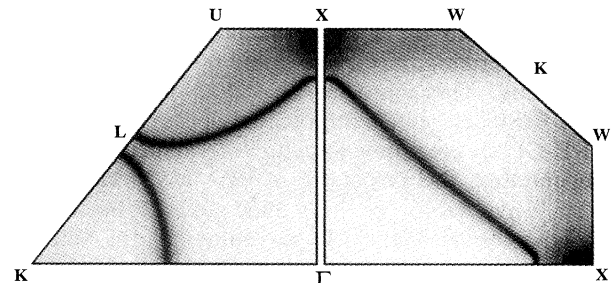


FIG. 1. The Fermi surface, i.e., $A_B(\mathbf{k}; \epsilon_F)$, for disordered CuPt for portions of the $\langle 1, 1, 0 \rangle$ (Γ - X - U - L - K), and $\langle 1, 0, 0 \rangle$ (Γ - X - W - K - W - X - L) planes. Spectral weight is given by relative grey scale, with black as largest and white as background. Note the neck at L and the smeared pockets at X .

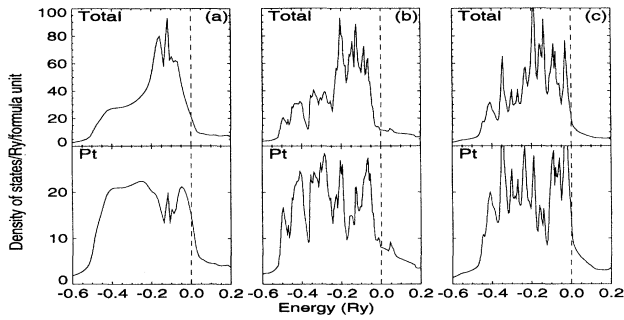


FIG. 2. Total densities of states for (a) disordered CuPt, using the scalar-relativistic KKR-CPA method; ordered CuPt in the (b) $L1_1$ and (c) $L1_0$ structures, using the scalar-relativistic LMTO method. The dashed line indicates the Fermi energy. Note the change of scale in partial Pt state densities.

The ordering mechanism described here is similar to the conventional Fermi-surface-nesting mechanism, in that both are examples of Bethe-Peierls instabilities. However, conventional Fermi-surface nesting takes place over extended regions of \mathbf{k} space between almost parallel sheets. The resulting structures tend to be long-period or incommensurate structures, since the spanning vector in general will be incommensurate with the lattice. In contrast, in the mechanism proposed here for CuPt, the spanning vector couples only the regions around the X and L points, and the large joint density of states results from van Hove singularities that exist near ϵ_F . This mechanism will naturally lead to high-symmetry structures with short periodicities, since the spanning vectors will tend to connect high-symmetry points.

Below a critical temperature, $S^{(2)}(\mathbf{q})$ indicates that a state with a concentration wave $\mathbf{q} = (\frac{1}{2}, \frac{1}{2}, \frac{1}{2})$ will lower the free energy of the disordered state. To confirm this, we calculated the total energy, bands, and densities of states for two ordered configurations using the linear muffin tin orbital method (LMTO) as well as the density of states for the disordered state [19].

In the disordered case, Fig. 2(a), ϵ_F cuts the top of the Pt d band, which is consistent with the X pockets in the Fermi surface. In the $L1_1$ structure, which can be viewed as an alloy with a $\mathbf{q} = (\frac{1}{2}, \frac{1}{2}, \frac{1}{2})$ concentration wave with unit amplitude, the density of states at ϵ_F is reduced, since the modulation in concentration introduces couplings between states at ϵ_F .

The $L1_0$ density of states in Fig. 2(c) demonstrates that not all ordered structures will produce this effect. The $L1_0$ structure corresponds to an alloy with $\mathbf{q} = (1, 0, 0)$ concentration wave with unit amplitude. The Fermi level still cuts a substantial amount of the d electron density of states, although smaller than for the disordered configuration. Figure 3 clearly shows the effect of periodicity in the ordered $L1_1$ structure, i.e., the couplings between the fcc X and L points. Whereas, in the ordered $L1_0$ structure, only couplings between two of the X points and Γ exist. A small Bethe-Peierls-type set

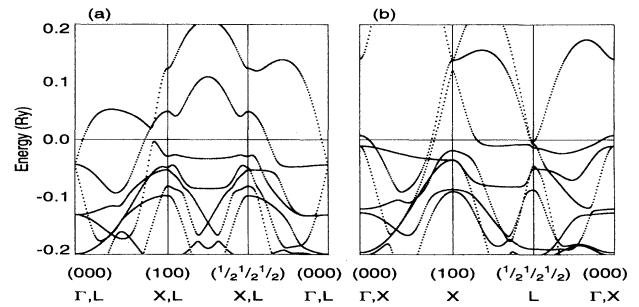


FIG. 3. LMTO CuPt band structure near ϵ_F for (a) $L1_1$ and (b) $L1_0$. The plots are along the same directions in reciprocal space, with indicated indices and symmetry points referring to the underlying fcc structure. Note the removal of degeneracy around (000) and $(\frac{1}{2}, \frac{1}{2}, \frac{1}{2})$ in $L1_1$.

of bonding and antibonding peaks exist in the $L1_1$ Pt d -state density in Fig. 2(b), with the bonding portion (of mixed X and L character) just below ϵ_F . Furthermore, the associated lowering of the energy is confirmed by the ordered-LMTO total-energy calculations. The $L1_0$ - $L1_1$ energy difference is 2.3 mRy per atom in favor of the $L1_1$ structure, which compares well with the 2.1 mRy energy difference found using a full-potential method [22].

There remains the question of the robustness of this mechanism. By lowering the " ϵ_F " (in a rigid-band fashion), thereby increasing the number of hole states at the X points, it should be more difficult for a $(\frac{1}{2}, \frac{1}{2}, \frac{1}{2})$ concentration wave to occupy these X pockets in the ordered state, so $L1_1$ ordering should not be favored. Indeed, calculations repeated with the Fermi level lowered by 30 mRy (into the Pt d -electron peak near ϵ_F , see Fig. 2) resulted in a large clustering tendency, which is dramatically increased with further reduction in ϵ_F . On the other hand, raising ϵ_F by 30 mRy, just above the Pt d -electron states in the random alloy in Fig. 2, gives peaks in $S^{(2)}(\mathbf{q})$ at all X points, indicating $L1_0$ -type ordering. By filling the hole pockets in the Pt d states of the disordered alloy, thereby removing the van Hove singularities at ϵ_F , there is no advantage by ordering into $L1_1$ over $L1_0$.

The above simple electron-per-atom arguments applied within a rigid-band approach may not be useful, however, for pointing to a suitable candidate to alter the ordering of CuPt to (100)-type ordering because such arguments are not valid when alloying late transition metals with noble metals, since both diagonal and off-diagonal disorder drive the ordering in such situations [10,23]. We find that the band-energy contribution alone favors $\mathbf{q} = (\frac{1}{2}, \frac{1}{2}, \frac{1}{2})$ ordering over a wide range of Pt concentration, and the inclusion of double-counting terms are required to obtain a change in ordering with concentration. Clearly, filling up the d holes is sufficient to change the fcc ordering tendency of CuPt.

While this novel Fermi-surface and van Hove-singularity mechanism is evident around 50% Cu, the $L1_2$ ordering to the Cu-rich side of the usual 75%

stoichiometry and the subsequent development of the one-dimensional LPS around 73% Cu [1] suggest that a conventional Fermi-surface mechanism is operable. Indeed, we find nested regions of Fermi surface in the (100) plane (see Fig. 1) associated with the s - p electrons, as found in Cu-rich Cu-Pd alloys [8]. The Fermi-surface dimensions are concentration dependent, and, at 73% Cu, Krivoglaz [24] construction suggests a peak in $\alpha(\mathbf{q})$ at $\mathbf{q} = (1, 0.2, 0)$, as we, in fact, find, provided *both* band-energy and double-counting terms are included. Thus, within the Cu-Pt system we find a crossover from a conventional Fermi-surface ordering mechanism around 75% Cu to ordering dominated by the novel van Hove-singularity-driven mechanism at 50%. As we progress to still higher Pt concentrations, we find that the ASRO for CuPt₃ has peaks at L with subsidiary peaks at X . The ordered tetragonal fcc-based superstructure of CuPt₃ is consistent with concentration waves associated with these \mathbf{q} vectors [5]. This interesting concentration dependence of the ordering tendency is the subject of a larger, more detailed paper.

Finally, we consider whether this unusual van Hove mechanism may play a role in other Pt alloy systems. The origins of $L1_0$ ordering in NiPt have been discussed elsewhere [10,23]. For both AgPt and AuPt, we find strong clustering tendencies (AuPt the largest, as seen experimentally), but with small accompanying peaks at $(\frac{1}{2}, \frac{1}{2}, \frac{1}{2})$ from a similar mechanism, with the AuPt satellite peak fairly small. Unfortunately, there is no solid solution AgPt phase to confirm this, and only a very narrow solid solution phase for AuPt [1]. (Perhaps with modern surface growth techniques, metastable $L1_1$ AgPt could be formed.) This indicates that CuPt is indeed unique in its electronic nature, hence the atypical $L1_1$ ordering [25]. Nonetheless, it is possible that the van Hove mechanism is in operation in other fcc systems, or other Bravais lattices. Since the mechanism naturally gives rise to structures with small unit cells, it would be interesting to identify structures which are not obviously stabilized by other mechanisms (e.g., electrostatics) to see if this effect may also be in operation there.

In summary, we have shown that the stability of the ordered CuPt structure (relative to the disordered state) originates from a novel mechanism which derives an ordering wave vector by connecting van Hove singularities at two high-symmetry points, the X and L points. In general, the mechanism will lead to simple ordered structures, like $L1_1$. At low temperatures, the $L1_1$ structure in CuPt is stabilized by filling the X -hole pockets. This requires a Bethe-Peierls-type mechanism to be active, which is confirmed by the ordered LMTO calculations. Because of the nature of the CuPt electronic structure, the $L1_1$ is uniquely observable in the CuPt system.

This work is supported in part by the U.S. Department of Energy at Sandia National Laboratories (by a New Initiative with OBES, Division of Materials) under Contract

No. DE-AC04-94AL85000, at Lawrence Livermore National Laboratory under Contract No. W-7405-ENG-48, and in part by the National Science Foundation under Contract No. DMR 9217297 and by the Ohio Supercomputer Centers.

-
- [1] *Binary Alloy Phase Diagrams*, edited by T. B. Massalski, H. Okamoto, P. R. Subramanian, and L. Kacprzak (American Society for Metals, Metals Park, OH, 1986), 2nd ed., p. 950.
 - [2] G. M. Stocks and H. Winter, *Z. Phys. B* **46**, 95 (1982).
 - [3] D. D. Johnson *et al.*, *Phys. Rev. B* **41**, 9701 (1990).
 - [4] D. D. Johnson *et al.*, *Phys. Rev. Lett.* **56**, 2088 (1986).
 - [5] A. Khachatryan, *Theory of Structural Transformations in Solids* (John Wiley and Sons, New York, 1983), Chap. 3, p. 556.
 - [6] K. Ohshima and D. Watanabe, *Acta. Crystallogr.* **29**, 520 (1973).
 - [7] D. D. Johnson and F. J. Pinski, *Phys. Rev. B* **48**, 11 553 (1993).
 - [8] B. L. Györffy and G. M. Stocks, *Phys. Rev. Lett.* **50**, 374 (1983).
 - [9] J. B. Staunton, D. D. Johnson, and F. J. Pinski, *Phys. Rev. B* **50**, 1450 (1994).
 - [10] D. D. Johnson, J. B. Staunton, and F. J. Pinski, *Phys. Rev. B* **50**, 1473 (1994).
 - [11] L. Onsager, *J. Am. Chem. Soc.* **58**, 1468 (1936).
 - [12] B. L. Györffy *et al.*, in *Alloy Phase Stability*, edited by G. M. Stocks and A. Gonis, NATO Advanced Studies Institute, Ser. E, Vol. 163 (Kluwer, Dordrecht, 1989), pp. 421-468.
 - [13] I. Masanskii, V. Tokar, and T. Grishchenko, *Phys. Rev. B* **44**, 4647 (1991).
 - [14] V. Gorsky, *Z. Phys.* **50**, 64 (1928).
 - [15] L. W. Bragg and E. J. Williams, *Proc. R. Soc. London A* **145**, 699 (1934).
 - [16] P. Clapp and S. Moss, *Phys. Rev.* **171**, 754 (1968).
 - [17] J. Staunton *et al.*, *Alloy Phase Stability* (Ref. [12]), pp. 469-508.
 - [18] W. Kohn and P. Vashita, in *Theory of the Inhomogeneous Electron Gas*, edited by S. Lundquist and N. H. March (Plenum, New York, 1983), p. 79.
 - [19] J. F. Clark *et al.*, in *Metallic Alloys: Experimental and Theoretical Perspectives*, edited by J. S. Faulkner and R. G. Jordan, NATO Advanced Studies Institute, Ser. E, Vol. 256 (Kluwer, Dordrecht, 1994), pp. 159-166.
 - [20] J. F. Clark, Ph.D. thesis, University of Cincinnati, 1993.
 - [21] F. Ducastelle, *Order and Phase Stability in Alloys, Series: Cohesion and Structure*, edited by F. R. de Boer and D. G. Pettifor (North-Holland, New York, 1991), Vol. 3, pp. 142, Fig. 3.44b.
 - [22] Z. W. Lu *et al.*, *Phys. Rev. B* **44**, 512 (1991).
 - [23] F. Pinski *et al.*, *Phys. Rev. Lett.* **66**, 766 (1991).
 - [24] M. A. Krivoglaz, *Theory of X-Ray and Thermal-Neutron Scattering by Real Crystals* (Plenum, New York, 1969).
 - [25] $L1_1$ ordering is found in other types of nonmetallic, or nonsubstitutional, compounds, such as nonstoichiometric carbides.

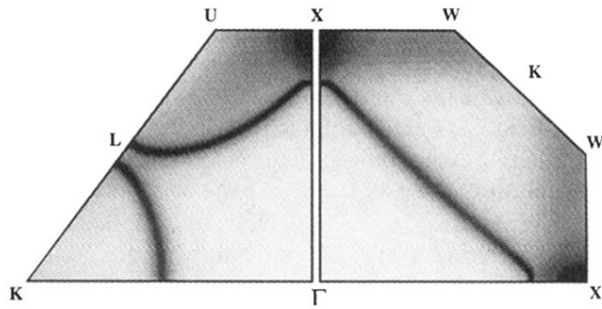


FIG. 1. The Fermi surface, i.e., $A_B(\mathbf{k}; \epsilon_F)$, for disordered CuPt for portions of the $\langle 1, 1, 0 \rangle$ (Γ -X-U-L-K), and $\langle 1, 0, 0 \rangle$ (Γ -X-W-K-W-X-L) planes. Spectral weight is given by relative grey scale, with black as largest and white as background. Note the neck at L and the smeared pockets at X.